

# Increasing Arctic River Discharge and Its Role for the Phytoplankton Responses in the Present and Future Climate Simulations

Junghyun Park<sup>1</sup>, Seong-joong Kim<sup>2</sup>, Hyung-Gyu Lim<sup>3</sup>, JONG-SEONG KUG<sup>4</sup>, Eun Jin Yang<sup>5</sup>, and Baek-Min Kim<sup>5</sup>

<sup>1</sup>Division of Earth Environmental System Science Major of Environmental Atmospheric Sciences, Pukyong National University, Busan 48513, South Korea

<sup>2</sup>Division of Atmospheric Sciences, Division of Ocean Sciences, Korea Polar Research Institute, 26 Songdomirae-ro, Incheon 21990, South Korea

<sup>3</sup>Atmospheric and Oceanic Sciences Program, Princeton University, Princeton, NJ 08540, USA

<sup>4</sup>Division of Environmental Science and Engineering, Pohang University of Science and Technology (POSTECH), Pohang 37673, South Korea

<sup>5</sup>Division of Ocean Sciences, Korea Polar Research Institute, 26 Songdomirae-ro, Incheon 21990, South Korea

November 24, 2022

## Abstract

Arctic amplification is known to accelerate the hydrological cycle in high-latitude landmass, which eventually leads to increased river discharge into the Arctic Ocean. However, the majority of climate models in Coupled Model Intercomparison Project 5 (CMIP5) tend to underestimate Arctic river discharge. This study elucidates the role of additional Arctic river discharge for the phytoplankton responses in the present and future climate simulations. In the present climate simulation, the additional freshwater input showed a decrease in the phytoplankton in spring due to the increasing sea ice, and in summer, it showed an increase in phytoplankton due to the surplus nitrate leftover from spring and induced vertical mixing. Similar processes occurred in future climate simulations. However, in those simulations, the major response region of phytoplankton to additional freshwater input was altered from the Eurasian Basin to the Canadian Basin and the East-Siberian Sea. This is because the current marginal ice zone in the Barents-Kara Sea, where phytoplankton mainly responds, moves toward the East-Siberian-Chukchi Sea. We suggest that Arctic river discharge is potentially an important contributing factor for Arctic ecosystems in both present and future climate that controls sea ice and nutrient distribution.

1     **Increasing Arctic River Discharge and Its Role for the Phytoplankton Responses in**  
2                                   **the Present and Future Climate Simulations**

3     **Junghyun Park<sup>1</sup>, Seong-Joong Kim<sup>2</sup>, Hyung-Gyu Lim<sup>3</sup>, Jong-Seong Kug<sup>4</sup>, Eun Jin Yang<sup>5</sup>**  
4     **and Baek-Min Kim<sup>1,\*</sup>**

5     <sup>1</sup>Division of Earth Environmental System Science Major of Environmental Atmospheric  
6     Sciences, Pukyong National University, Busan 48513, South Korea

7     <sup>2</sup>Division of Atmospheric Sciences, Division of Ocean Sciences, Korea Polar Research Institute,  
8     26 Songdomirae-ro, Incheon 21990, South Korea

9     <sup>3</sup>Atmospheric and Oceanic Sciences Program, Princeton University, Princeton, NJ 08540, USA

10    <sup>4</sup>Division of Environmental Science and Engineering, Pohang University of Science and  
11    Technology (POSTECH), Pohang 37673, South Korea

12    <sup>5</sup>Division of Ocean Sciences, Korea Polar Research Institute, 26 Songdomirae-ro, Incheon  
13    21990, South Korea

14    Corresponding author: Baek-Min Kim (baekmin@pknu.ac.kr)

15    **Key Points:**

- 16       • Additional river discharge in the present climate increases Arctic sea ice and decreases  
17       surface phytoplankton in spring.
- 18       • The surplus nutrients due to the decrease of phytoplankton in the spring increase the  
19       surface phytoplankton in the summer.
- 20       • The present phytoplankton hotspot in the Eurasian Basin shifts to the Canadian Basin in  
21       the future climate simulation.

22 **Abstract**

23 Arctic amplification is known to accelerate the hydrological cycle in high-latitude landmass,  
24 which eventually leads to increased river discharge into the Arctic Ocean. However, the majority  
25 of climate models in Coupled Model Intercomparison Project 5 (CMIP5) tend to underestimate  
26 Arctic river discharge. This study elucidates the role of additional Arctic river discharge for the  
27 phytoplankton responses in the present and future climate simulations. In the present climate  
28 simulation, the additional freshwater input showed a decrease in the phytoplankton in spring due  
29 to the increasing sea ice, and in summer, it showed an increase in phytoplankton due to the  
30 surplus nitrate leftover from spring and induced vertical mixing. Similar processes occurred in  
31 future climate simulations. However, in those simulations, the major response region of  
32 phytoplankton to additional freshwater input was altered from the Eurasian Basin to the  
33 Canadian Basin and the East-Siberian Sea. This is because the current marginal ice zone in the  
34 Barents-Kara Sea, where phytoplankton mainly responds, moves toward the East-Siberian-  
35 Chukchi Sea. We suggest that Arctic river discharge is potentially an important contributing  
36 factor for Arctic ecosystems in both present and future climate that controls sea ice and nutrient  
37 distribution.

38

39 **Plain Language Summary**

40 Arctic warming is known to accelerate hydrologic cycles at high latitudes. However, most  
41 climate models still underestimate river discharges into the Arctic Ocean compared to real world.  
42 Our research studies the impact of increasing river discharge on phytoplankton in the present and  
43 future climates using the earth system model. In the present climate, increased river discharge  
44 reduces phytoplankton in spring and increases it in summer. Additional river discharge in spring  
45 increases sea ice and decreases phytoplankton. However, the limited growth of phytoplankton  
46 preserves nutrients during spring, and therefore, leads to explosive phytoplankton growth in  
47 summer. In the future climate, as in the present climate, phytoplankton in spring decreases, and  
48 phytoplankton in summer increases. However, the major response region moves from the  
49 Eurasian to the Canadian Basin. We suggest that Arctic river discharge is potentially an  
50 important contributing factor for Arctic ecosystems in both present and future climate by  
51 influencing sea ice and nutrient distribution.

52 **1 Introduction**

53 Arctic warming is one of the most remarkable phenomena in global surface temperature  
54 changes (Cohen et al., 2014) causing sea ice melting due to increased atmospheric carbon  
55 dioxide concentration and increased downward longwave radiation (Comiso, 2003; Serreze et al.,  
56 2007; Maslanik et al., 2007), and enhancing a strong positive feedback, e.g., ice-albedo feedback  
57 (Perovich et al., 2007; Holland et al., 2010; Kashiwase et al., 2017). The more remarkable  
58 temperature rise in the Arctic region compared to the other regions, often called Arctic  
59 amplification (AA), has influenced not only Arctic climate itself such as Arctic moistening (Min  
60 et al., 2008) and marine acidification (Terhaar et al., 2020), but imposes a remote impact via  
61 modulating and atmospheric circulation patterns onto the region with high human populations in  
62 the tropics and mid-latitudes (Kim et al., 2014; Kug et al., 2015; Coumou et al., 2018; Kennel &  
63 Yulaeva, 2020) . As AAs are projected to become stronger in the future scenarios established by  
64 Coupled Model Intercomparison Project (CMIP) models, it is of utmost importance to  
65 understand the Arctic environment and ecosystem changes due to the current and future  
66 accelerating warming (Smith et al., 2019).

67 Recent studies suggested that Arctic warming can be amplified by changes in marine  
68 phytoplankton biomass (Park et al., 2015; Lim et al., 2019a, b) and human-induced nitrogen flux  
69 from river discharge and atmospheric depositions in the future climate (Lim et al., 2021). The  
70 reduction of sea ice extent and its thickness allows more penetrations of shortwave radiation into  
71 the Arctic Ocean surface (Perovich et al., 2011; Nicolaus et al., 2012; Arrigo et al., 2014) that  
72 triggers the earlier bloom timing in marine phytoplankton at the edge of sea ice (Frey et al.,  
73 2015) and sub-ice bloom (Arrigo et al., 2012, 2014; Horvat et al., 2017). The increased  
74 phytoplankton biomass leads to heat redistribution in ocean layers via modulating attenuation

75 coefficients (Morel, 1988; Manizza & Que, 2005) that may influence the simulated AA (Park et  
76 al., 2015; Lim et al., 2019a, b; Lim et al., 2021). This new mechanism to understand the possible  
77 positive feedback highlights the role of the Arctic ecosystem in terms of air-sea-biogeochemical  
78 interactions, which may be overlooked in future Arctic projections using Earth System Models  
79 (ESMs).

80         Lewis et al. (2020) showed that the primary productivity of the Arctic Ocean increased  
81 by 30 % from 1998 to 2012, owing to the expansion of open water. Since then, primary  
82 productivity has exhibited an increasing trend in general because of increased phytoplankton.  
83 Future projections of the primary productivity of the Arctic Ocean simulated in CMIP5 models  
84 suggested large uncertainties, mainly depending on nitrate storage (Vancoppenolle et al., 2013).  
85 Ardyna & Arrigo (2020) suggested that the shelf-break, serving as a “green belt,” can effectively  
86 supply inorganic and organic materials to increase marine productivities in the stratified Arctic  
87 Ocean.

88         Arctic Ocean warming alters hydrologic and oceanic circulations, such as sea ice melting,  
89 intensified precipitation (Min et al., 2008), and increased river discharge (Haine et al., 2015). In  
90 particular, while the Arctic Ocean accounts for 1 % of the global volume of the ocean, it receives  
91 more than 10 % of the global river discharge (McClelland et al., 2012). Notably, long-term  
92 changes in river discharge have been steadily increasing. In particular, Eurasian river discharge  
93 in 2018 was 12 % greater than the average for 1980–1989 (Peterson et al., 2002; Holmes et al.,  
94 2018). In addition, river discharge under the future climate conditions is projected to increase by  
95 more than 50 % compared to the present, mainly in Alaska and Siberia (Bring et al., 2017).  
96 However, in the CMIP5 models, the surface salinity around the river is overestimated because of  
97 the underestimation of river discharge with large uncertainties (Shu et al., 2018).

98           Several recent observational studies have reported that Arctic river discharge modulates  
99 Arctic biogeochemistry by delivering dissolved organic matter that enhances phytoplankton  
100 response (Holmes et al., 2012; Fichot et al., 2013; Tremblay et al., 2014; Ardyna et al., 2017).  
101 However, it is difficult to independently analyze the impact of additional river discharge on the  
102 marine ecosystems of the Arctic Ocean in observational studies, and studies on ESMs to clarify  
103 if these are insufficient. In addition, it is challenging to predict future Arctic ecosystems because  
104 of the uncertainty of the primary productivity simulated by models (Vancoppenolle et al., 2013;  
105 Ardyna & Arrigo, 2020).

106           In this study, we used the ESM to study the sensitivity of phytoplankton to additional  
107 river discharge in the present and future climate simulation. Our model simulation outputs  
108 suggest that Arctic river discharge can control sea ice and nutrient distribution, which are factors  
109 that affect phytoplankton growth. We outlined the mechanisms by which additional river  
110 discharges under the influence of present climate conditions affect spring and summer sea ice  
111 melting and nutrient distribution. In addition, we analyzed the impact of increased river water  
112 discharge under the influence of future climate conditions on future Arctic ecosystems, thus  
113 highlighting the importance of river discharge on ecosystem changes in the future.

## 114 **2 Materials and Methods**

### 115           2.1 GFDL-CM2.1-TOPAZ2

116           In this study, we applied the ESM named GFDL CM2.1, coupled with the  
117 biogeochemical model Tracers of Ocean Phytoplankton with Allometric Zooplankton code  
118 version 2.0 (TOPAZv2; Griffies et al., 2005; Dunne et al., 2012, 2013). GFDL-CM2.1-TOPAZ  
119 consists of an atmospheric model (AM2), land model (LM2), modular ocean model (MOM5),  
120 sea ice simulator (SIS), and ocean biogeochemistry model (TOPAZv2). The AM2 and LM2

121 horizontal resolutions are  $2^\circ$  latitude  $\times$   $2.5^\circ$  longitude, and the vertical resolution of AM2 is 24  
122 levels grid. MOM5 uses a tripolar grid to remove the spherical coordinate singularity of the  
123 Arctic Ocean. below the Arctic north of  $65^\circ$  N, and above it switches to a bipolar region with  
124 coordinate singularities over Siberia and Canada. MOM5 and SIS horizontal resolutions are  $1^\circ$  in  
125 the extratropics, with finer meridional grid-spacing in the tropics ( $\sim 1/3^\circ$ ). The vertical resolution  
126 of MOM5 is 50 levels grid, with 22 evenly spaced levels over the top 220 m (Griffies et al.,  
127 2005).

128 TOPAZv2 considers the cycle of carbon, and nutrients such as nitrogen, phosphorus,  
129 silicon, and iron (Dunne et al., 2013). The phytoplankton is calculated by dividing it into three  
130 groups, i.e., small, large, and nitrogen-fixing diazotrophs. The phytoplankton growth rate is  
131 calculated as a function of various chlorophyll to carbon ratios and is limited by nutrients and  
132 light (Dunne et al., 2010). TOPAZv2 includes external inputs from atmospheric nitrogen  
133 deposition lithogenic dust, soluble iron, and river nitrogen. For more detailed information, see  
134 Dunne et al. (2013).

135 In GFDL-CM2.1-TOPAZ, river discharge is controlled in the land module. The total  
136 water storage (W) of LM2 consists of each non-glaciated cell composed of a snowpack store, a  
137 root-zone store, a groundwater store, and a glaciated cell composed of a snowpack and a glacier-  
138 ice store. Each water store has a different equation for water balance; see Milly & Shmakin  
139 (2002) for details. River discharge is the total amount of water from land to the sea. In this  
140 model, the river discharge is calculated as the sum of groundwater, melted water from glaciers  
141 and snow, and any rainfall immediately combined with melted water. To inflow additional  
142 freshwater in our study, we add a freshwater control term to this calculation.

143 2.2 Experiment

144 To analyze the changes in phytoplankton due to the additional river discharge in the  
145 present and future climates, we performed four experiments by simulating the present and future  
146 climates and controlling the river discharge in each condition. We used abbreviations to  
147 distinguish between each experiment. The freshwater addition experiments were abbreviated as  
148 “FWadd,” and the standard experiments were abbreviated as “CTRL.” In addition, to distinguish  
149 between the present and future climate simulations, we used parentheses after each experimental  
150 abbreviation to indicate the present and future with uppercase P and capital F, respectively [e.g.,  
151 CTRL(P), FWadd(F)].

152 The present climate simulation was performed similarly to the 1990 level experiment,  
153 which is often used as the present experiment in previous studies using the CM2.1 model  
154 (Gnanadesikan et al., 2006; Delworth et al., 2012; Lim et al., 2019a, b). The present climate  
155 simulation is performed by prescribing greenhouse gases, such as carbon dioxide, methane, and  
156 nitrous oxide, as well as organic and inorganic nitrogen oxides prescribed for rivers and  
157 atmosphere at 1990 levels (Green et al., 2004; Hegglin et al., 2016).

158 The future climate simulation set twice as much carbon dioxide as the present condition  
159 to simulate the future climate. The future climate simulation (F) performed calculations for 110  
160 years with 706 ppm carbon dioxide, increasing by 1 % from the present climate condition.  
161 Before performing the freshwater addition experiments, we performed a 1200-year spin-up to  
162 make an environment for the present climate and the future climate, respectively.

163 The freshwater addition experiments were based on the water-hosing experiment  
164 performed in the Paleoclimate Modeling Intercomparison Project 2 (PMIP2; Stouffer et al.,  
165 2006). In existing literature that adopted water-hosing experiments, additional water was

166 uniformly added to 50–70° N latitudes for 100 years to study vertical currents (Yin & Stouffer,  
167 2007; Kim & An, 2019). In this study, the freshwater addition experiments were performed by  
168 simulating the addition of freshwater to the river discharge of the entire Arctic Ocean at latitude  
169 65–90° N.

170 In the freshwater addition experiments, if the integration time is prolonged, the sea  
171 surface height continues to increase, which may cause water balance problems (Fig. S1).  
172 Therefore, for the integration time, a 70-year integration was performed, while considering the  
173 level that does not destroy the mass balance; only the last 30 years were analyzed considering the  
174 spin-up time of the model.

### 175 2.3 Additional river discharge forcing

176 We set the additional river discharge at 0.03 Sv (1 Sv =  $10^6$  m<sup>3</sup>/s), the level of  
177 underestimated CMIP5 for Arctic river discharge, in the sum of all river discharge flowing into  
178 the Arctic Ocean. Shu et al. (2018) compared the CMIP5 model outputs and observation data for  
179 the hydrologic cycle. The river discharge averaged the CMIP5 model outputs of the present  
180 climate was  $0.083 \pm 0.036$  Sv, which is underestimated by approximately 0.021 Sv, compared to  
181 the observation data of  $0.102 \pm 0.004$  Sv. In addition, the simulated river discharge uncertainty  
182 of CMIP5 was approximately 0.036 Sv. From the above consideration, we set 0.03 Sv as an  
183 additional freshwater quantity.

184 We used the observational river discharge data provided by Arctic Great River  
185 Observatory (ArcticGRO) to compare the estimations from model output (Shiklomanov et al.,  
186 2021). ArcticGRO, initiated in 2002 by the Pan-Arctic River Transport of Nutrients, Organic  
187 Matter, and Suspended Sediments (PARTNERS) project, is part of a river observation project  
188 that collects and analyzes time-series water samples from six large rivers. The ArcticGRO uses

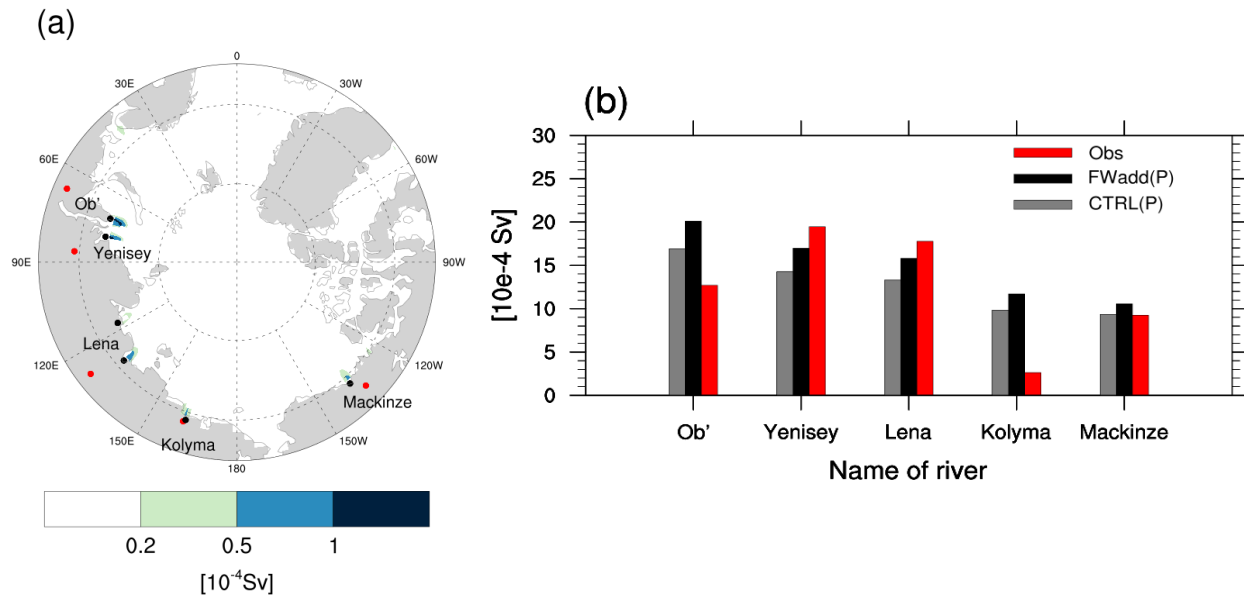
189 river discharge data from various hydrologic agencies, including near-real-time data. The  
190 LoadRunner software package is used to generate continuous daily discharge data, using  
191 calibrated regression from time series sampling observations (Booth et al., 2007). In this study,  
192 among the wide ArcticGRO river data, we compared data from five major rivers that flow into  
193 the Arctic Ocean, namely, Ob', Yenisey, Lena, Kolyma, and Mackenzie with model outputs. The  
194 analysis period of the river observation data averaged from 1981 to 2010 according to the present  
195 level.

196         The position of the simulated river mouth was similar to the observation point. Figure  
197 1(a) portrays the 1000-year average river discharge for the CTRL(P). The black dots mark the  
198 river mouth simulated by the model, while the red dots are the observation points. By comparing  
199 each point, we found that the simulated river mouth position in the model did not appear to  
200 deviate significantly from the observation point. In addition, river discharge was mainly in East-  
201 Siberia and the Laptev Sea.

202         The amounts of river discharge in each mouth, indicated by dots in Figure 1(a), were  
203 compared to those in Figure 1(b). The gray box indicates the 1000-year average river discharge  
204 of CTRL(P), the black box indicates the river discharge added by 0.03 Sv to the 1000-year  
205 average river discharge of CTRL(P), and the red box indicates the observation data. Note that we  
206 are analyzing model data for qualitative comparison with observation data, and as most of the  
207 observation data is a regression by a statistical model, caution is required in interpretation.

208         Significant amount of river discharge flowed from the large rivers Lena, Yenisey, and  
209 Ob', as designed in the FWadd experiment. The model simulated river discharge was the largest  
210 in the Ob River in the Arctic, unlike the observation data. In addition, the simulated river  
211 discharge was overestimated in the Ob' and Kolyma rivers and underestimated in the Yenisey

212 and Lena rivers. However, except for the Kolyma River, the discharge was within a relatively  
 213 acceptable range.

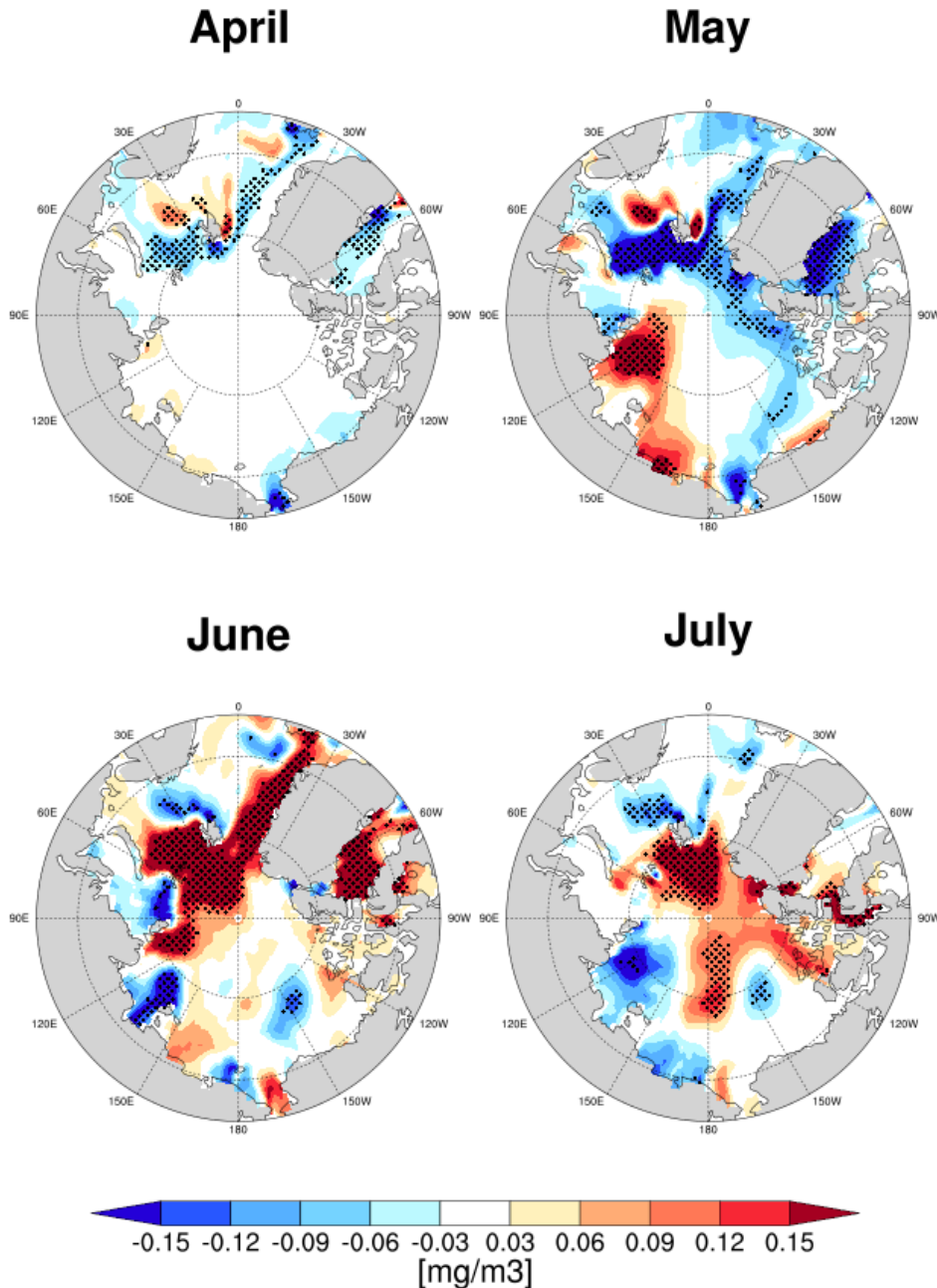


214 **Figure 1.** Comparison of annual mean river discharge of CTRL(P), FWadd(P), and observation  
 215 (Obs). (a) 1000-yr annual mean river discharge of CTRL(P) (shaded). The black dots are the  
 216 simulated five largest river mouths of the models. The red dots indicate the sites of observation  
 217 (ArcticGRO). (b) The amount of river discharges at the mouth of each of five rivers.

### 218 3 Results

#### 219 3.1 Impact of river discharge in the present climate simulation

220 In the present climate simulation, the overall response of phytoplankton to additional  
 221 river discharge results in a decrease in the phytoplankton in spring and an increase in summer.  
 222 Figure 2 shows the anomaly by averaging the upper ocean (0–20 m) chlorophyll  
 223 concentrations—representing the phytoplankton—between the CTRL(P) and FWadd(P)  
 224 experiments in spring (April, May) and summer (June, July). Note that chlorophyll concentration  
 225 refers to the biomass of phytoplankton.



226

227 **Figure 2.** Impact of increased river discharge in spring (April–May) and summer (June–July) in  
 228 the upper ocean (0–20 m) on chlorophyll concentration in the present climate simulation. The  
 229 shaded area indicates the difference between FWadd(P) and CTRL(P) of the chlorophyll  
 230 concentration. Black dots represent significant values of chlorophyll concentration at 95 %  
 231 confidence level.

232

In the present climate simulation, we found that an increase in river discharge in spring

233

can cause a decrease in phytoplankton, except in some areas. As for the anomaly pattern of

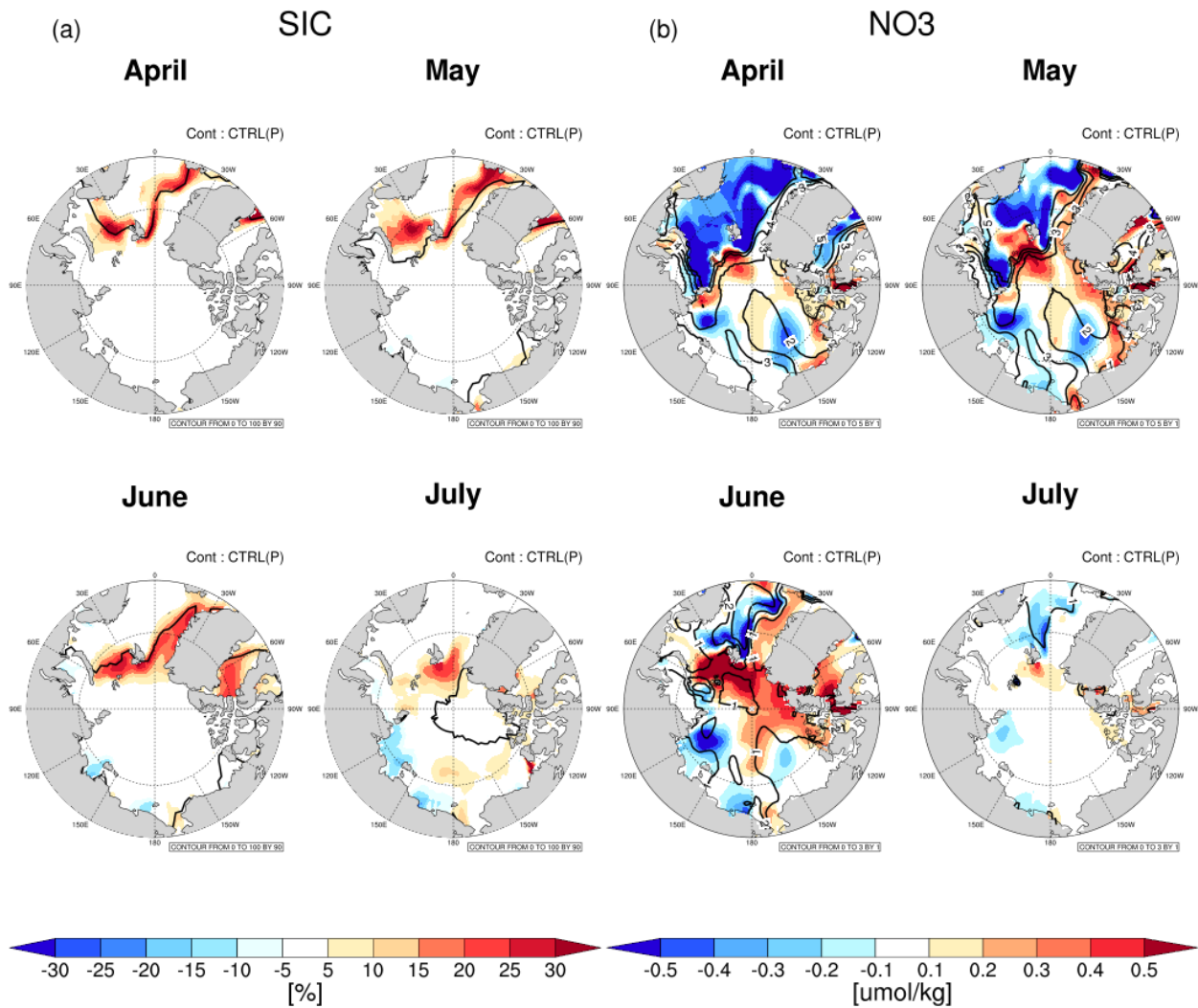
234

chlorophyll concentration in April, a negative anomaly pattern appeared in the Bering Strait,

235 Greenland Sea, and some areas of the Eurasian Basin (Fig. 2). In May, the anomaly pattern was  
236 similar to that in April, but with a more robust response. Most negative anomaly patterns in April  
237 and May appeared in the area in contact with the surrounding ocean. These results suggest that  
238 limiting factors restraining phytoplankton growth have developed near the border between the  
239 surrounding and Arctic oceans.

240 An increase in river discharge leads to a decrease in the surface salinity and surface  
241 temperature of the Arctic Ocean, thus, increasing the sea ice concentration in the region (Fig. S2;  
242 Fig. 3a). The decrease in surface salinity was not limited to estuaries but was also observed in the  
243 Barents Sea, where sea ice variability was relatively large. In addition, an increase in river  
244 discharge resulted in a decrease in the inflow of the surrounding ocean due to an increase in sea  
245 surface height (SSH). These results are consistent with other model experiments that examined  
246 additional river discharge in the Arctic Ocean (Nummelin et al., 2016).

247



248

249 **Figure 3.** Changes in the limiting factors (SIC and NO<sub>3</sub>) of phytoplankton simulated by the  
 250 model in spring and summer. (a) Difference between FWadd(P) and CTRL(P) of sea ice  
 251 concentration (SIC)(shaded) and the averaged sea ice extent (SIC>15%) on CTRL(P)(contour).  
 252 (b) Difference between FWadd(P) and CTRL(P) of nitrate concentration (NO<sub>3</sub>) (shaded) and the  
 253 averaged NO<sub>3</sub> on CTRL(P)(contour).

254

In the present climate, an increase in summer river discharge may cause an increase in  
 255 phytoplankton, particularly in the Eurasian Basin (Fig. 2). A robust positive anomaly pattern  
 256 appeared in the June chlorophyll concentration anomaly pattern in the Barents Sea, Eurasian  
 257 Basin, and the Baffin Bay. As for the anomaly pattern of chlorophyll concentration in July, a  
 258 positive anomaly pattern appeared in the Eurasian and Makarov basins, as the pattern moved to

259 the center of the Arctic Ocean compared with its position in June. Notably, the positive anomaly  
260 pattern in June mainly appeared in the negative anomaly pattern in May. These results suggest  
261 that the reduction in phytoplankton due to spring sea ice melting affects the growth of  
262 phytoplankton in summer.

263 In summer, the limiting factor for phytoplankton growth is the depletion of nitrate, the  
264 primary nutrient for phytoplankton (Kattner & Budéus, 1997). The growth of spring  
265 phytoplankton, called a “chlorophyll bloom,” consumes nitrate, leading to nitrate depletion in the  
266 summer ocean (Lim et al., 2019a). Increased freshwater increases the sea ice concentration,  
267 thereby slowing down the chlorophyll bloom and reducing nutrient depletion (Fig. S3; Fig. 3a).  
268 Figure 3b shows the April–July anomaly by averaged nitrate concentration between the CTRL(P)  
269 and FWadd(P) experiments. This indicates that the positive anomaly pattern of nitrate  
270 concentration in June and July was nearly consistent with the positive anomaly pattern of  
271 phytoplankton. These results indicate that increased nitrate levels due to the increase in summer  
272 freshwater promoted the growth of phytoplankton.

273 We found that the summer nitrate increase in the FWadd experiment was associated with  
274 poor spring phytoplankton growth, and the negative anomaly pattern of chlorophyll  
275 concentration in May (Fig. 2) was similar to the positive anomaly pattern of nitrate concentration  
276 in June (Fig. 3b). Consistent with this pattern, phytoplankton, which did not grow well due to  
277 increased sea ice in the FWadd experiment, had lower spring nutrient consumption. Relatively  
278 low nutrient consumption promoted the growth of summer phytoplankton. Below the upper  
279 ocean layer (0–20 m), there was a decrease in phytoplankton because as the upper layers became  
280 nutrient-rich in summer, the subsurface chlorophyll maximum depth became shallow (Fig. S3).

281 Another reason for the increase in nitrate could be the increased summer sea ice.  
282 Sufficient summer light and shallow sea ice do not limit the light required for phytoplankton  
283 growth. However, in the process of sea ice formation, the ocean mixed layer depth under the  
284 salty sea ice deepens, owing to the brine rejection process (Peralta-Ferriz & Woodgate, 2015).  
285 This mechanism causes vertical mixing within the deep ocean, increases the nutrient levels, and  
286 may affect phytoplankton growth.

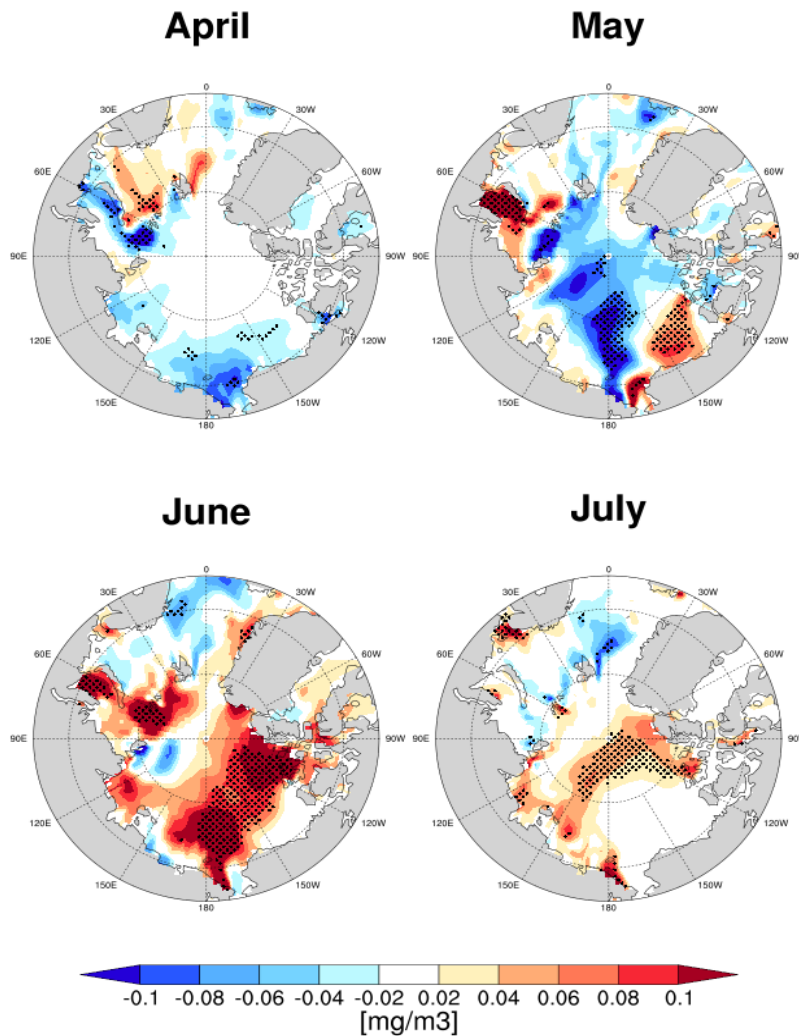
287 In the FWadd experiment, brine rejection occurred in summer in the Eurasian Basin (Fig.  
288 S4). Even though brine rejection did not appear in the entire area that experienced increased sea  
289 ice, brine rejection appeared near the Eurasian Basin, which is relatively far from the estuary,  
290 indicating a positive salinity anomaly. As a result, the mixed layer depth around the Eurasian  
291 Basin increased. This mechanism may be responsible for the substantial increase in nitrate levels,  
292 especially in the Eurasian Basin.

### 293 3.2 Impact of river discharge on future

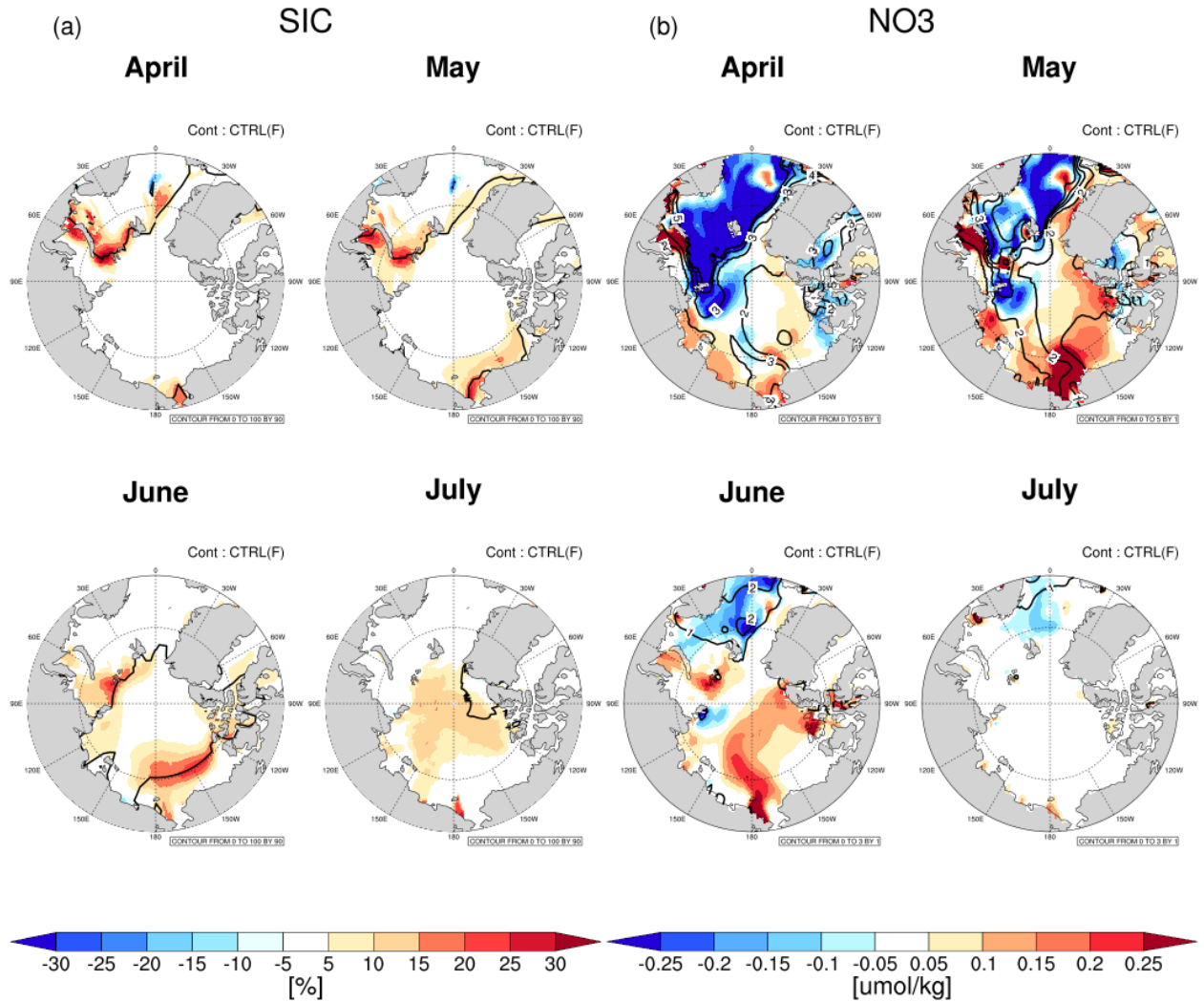
294 In the previous subsection, we reported on analysis of the effects and mechanisms of  
295 additional river discharge on phytoplankton in present climates. In this subsection we report on  
296 the analysis of the impact of additional river discharge on phytoplankton in the future climate  
297 simulation. In this simulation, the significant response of phytoplankton to additional river  
298 discharge showed a decrease in spring and an increase in summer, similar to that observed in the  
299 present climate simulation. However, while the changes in phytoplankton in the present climate  
300 appeared mainly in the Eurasian Basin, they extended to the Canada Basin in the future climate.

301 Figure 4 shows the upper ocean chlorophyll concentration anomaly between CTRL(F)  
302 and FWadd(F) in spring and summer. Notably, the future Arctic Ocean is expected to become  
303 more stratified under the future climate conditions compared to the present climate conditions by

304 melting ice and strengthening the hydrological cycle (Haine et al., 2015). Most models project  
305 that, in the future, surface nitrate concentrations will decrease due to the stratification of the  
306 Arctic Ocean (Vancoppenolle et al., 2013). The CTRL(F) results are consistent with the above-  
307 mentioned previous studies; the simulation showed a significant decrease in surface nitrate and  
308 phytoplankton levels compared to the CTRL(P).



309 **Figure 4.** Impact of increased river discharge in spring (April–May) and summer (June–July)  
310 upper ocean (0–20 m) on chlorophyll concentration in the future climate simulation. The shaded  
311 area indicates the difference between FWadd(F) and CTRL(F) of chlorophyll concentration.  
312 Black dots represent significant values of chlorophyll concentration at 95 % confidence level.  
313 Note that the future climate simulation was applied by adjusting the minimum and maximum  
314 values of the shading bar used in the present climate to approximately 70 %.



315 **Figure 5.** Changes in the limiting factors (SIC and NO<sub>3</sub>) of phytoplankton simulated by the  
 316 future in spring and summer. (a) Difference between FWadd(F) and CTRL(F) of sea ice  
 317 concentration (SIC)(shaded) and the averaged sea ice extent (SIC>15%) on CTRL(F)(contour).  
 318 (b) Difference between FWadd(F) and CTRL(F) of nitrate concentration (NO<sub>3</sub>) (shaded) and the  
 319 averaged NO<sub>3</sub> on CTRL(F)(contour). Note that the future climate simulation of nitrate  
 320 concentration was applied by adjusting the minimum and maximum values of the shading bar  
 321 used in the present climate to approximately 50 %.

322 In the future climate simulation, the increase in river discharge in spring resulted in a  
 323 negative anomaly of chlorophyll concentration. In addition, similar to the mechanism in the  
 324 present climate, the decrease in the phytoplankton biomass in response to sea ice increased.  
 325 However, compared with the results of the present climate simulations, negative anomaly

326 patterns appeared in the Kara and Chukchi seas, which are generally close to the interior of the  
327 Arctic Ocean.

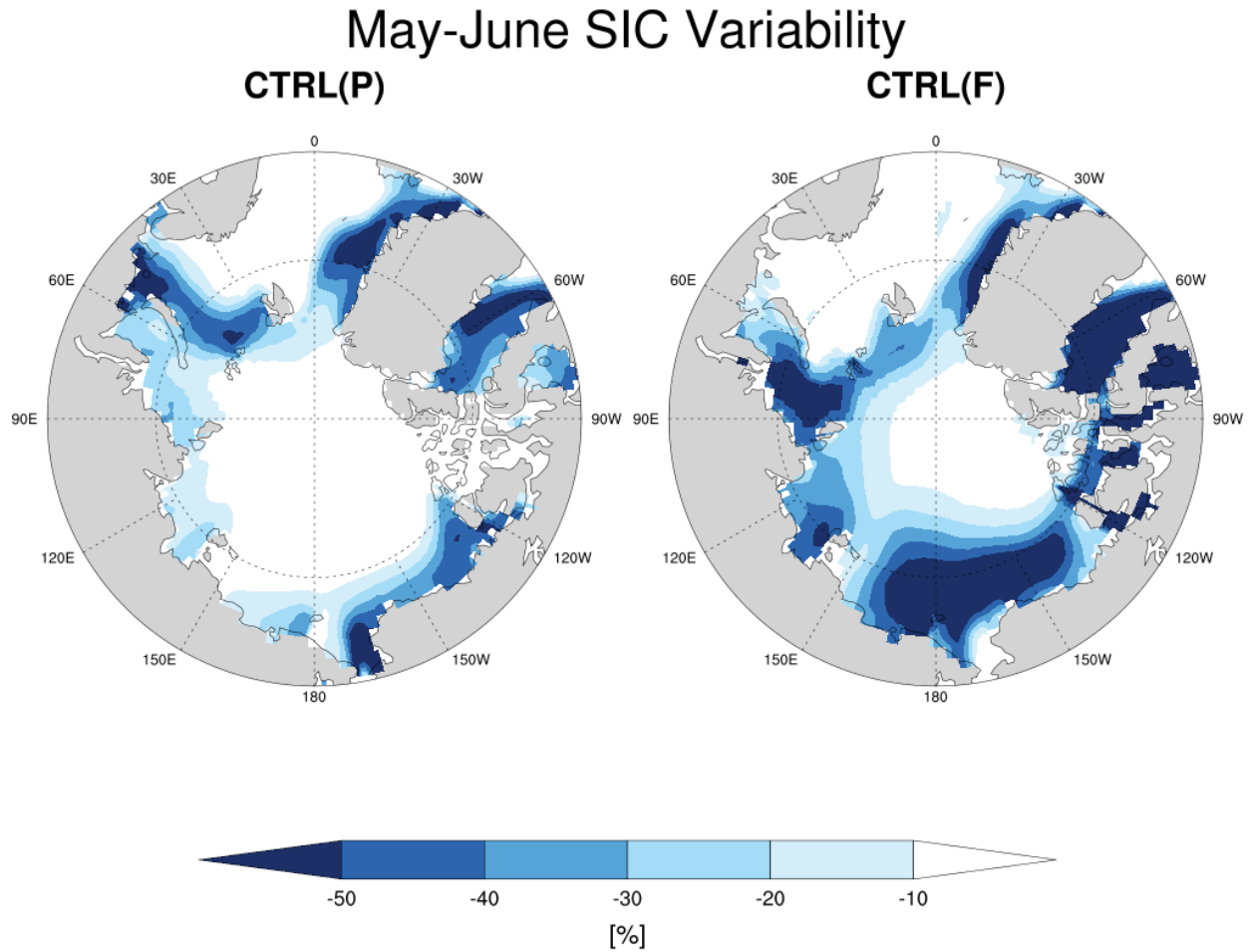
328 Figure 5a shows the average sea ice concentration anomaly between CTRL(F) and  
329 FWadd(F) during April–July. The positive anomaly pattern of sea ice concentration appears  
330 similar to the negative anomaly pattern of phytoplankton. The consistency of this pattern  
331 indicates a decrease in phytoplankton due to light blocked by increased sea ice, similar to the  
332 present climate simulation. However, in the future climate simulation, the sea ice extent was  
333 significantly reduced compared to the present climate simulation, resulting in broader negative  
334 anomaly patterns of phytoplankton. The mechanism of sea ice formation by freshwater was the  
335 same as that in the present climate simulation (Fig. S2).

336 The seasonal evolution of the marginal ice zone from May to June is remarkably different  
337 between the present and future climates (Fig. 6). In the present climate, the difference in sea ice  
338 concentration between May and June is significant in the Eurasian Basin with the Barents-Kara  
339 Sea. In contrast, more extensive sea ice fluctuations appear in the Beaufort and East-Siberian-  
340 Chukchi Sea in the future climate. These results suggest that future sea ice distribution changes  
341 may shift summer phytoplankton hotspots.

342 An increase in river discharge in future climate simulation caused an increase in summer  
343 phytoplankton similar to that in the present climate simulation; a response in the Canada Basin  
344 appeared broader and larger than in Eurasian Basin (Fig. 4). In June, the main anomaly pattern of  
345 chlorophyll concentration is the positive anomaly in the Eurasian Basin, Canada Basin, and East-  
346 Siberian-Chukchi Sea. However, the positive anomaly in the Eurasian Basin was narrow, while  
347 the anomaly in the Canadian Basin was wide. In July, the anomaly intensity weakened, and the  
348 pattern shifted toward the center of the Arctic Ocean, relative to that in June.

349            Unlike in the present, in the future climate simulation, summer nutrient changes due to  
350 additional river discharge were only related to spring phytoplankton blooming. Figure 5b shows  
351 the differences in the nutrients between CTRL(F) and FWadd(F). The nitrate positive anomaly  
352 pattern in June was similar to that of the chlorophyll concentration negative anomaly pattern in  
353 May, which showed the same mechanism as the present climate simulation. The consistency of  
354 this anomaly pattern implies that freshwater-induced spring sea ice increases contribute to  
355 summer phytoplankton growth, even in the future climate simulation.

356            The mechanism of the nutrient increase caused by brine rejection is weakened in future  
357 simulations (Fig. S4). Excessive stratification of the Arctic Ocean and additional river discharge  
358 lowers the ocean salinity when the sea ice freezes, with relatively little brine left behind within  
359 the sea ice. The decrease in the salinity within the sea ice reduces the increase in salinity caused  
360 by brine rejection in the Eurasian Basin in present climates. For this reason, the vertical mixing  
361 induced by brine rejection is weakened, and ocean stratification due to the addition of river  
362 discharge becomes stronger.



363 **Figure 6.** Changes in the May-June marginal ice zone in the present and future climate  
364 experiments. The left figure shows the difference in sea ice concentration in May and June in  
365 CTRL(P). The right figure shows the difference in sea ice concentration in May and June in  
366 CTRL(F).  
367

#### 368 **4 Summary and Discussion**

369         We studied the mechanism by which the increase in Arctic river discharge—  
370 underestimated in most models—affects spring and summer phytoplankton in the present and  
371 future climates. In the present climate simulation, additional river discharge in spring decreased  
372 the phytoplankton biomass near the Eurasian Basin due to the light blocked by increased sea ice.  
373 In summer, additional river discharge increased the phytoplankton biomass, mainly in the  
374 Eurasian Basin, as indicated by the nutrients not consumed in the spring and the vertical mixing

375 caused by brine rejection. In the future climate simulation, similar to the present climate  
376 simulation, phytoplankton decreased in spring due to increased sea ice. In addition, although an  
377 increase in phytoplankton appeared in the summer, it strongly emerged in the Canada but not in  
378 the Eurasian Basin. We suggest that the shift of the significant response region of phytoplankton  
379 in future climates is largely controlled by future sea ice distribution.

380         The comparison between observational and model data performed in the Method Section  
381 is a qualitative comparison, and it is not necessary to focus on the quantitative differences  
382 between these results. Actually, direct comparison with observation might not be possible in this  
383 case. As described in the Result Section, the phytoplankton response mainly occurred over the  
384 marginal sea-ice zone far from the freshwater source region. Therefore, our interpretation would  
385 still be valid even if different spatial patterns of river discharge were simulated by the model.

386         Previous studies have revealed that future phytoplankton can enhance the AA (e.g., Park  
387 et al., 2015). It has been suggested that phytoplankton blooming in early spring could enhance  
388 positive feedback by ice-albedo and biogeophysical feedback (Lim et al., 2019a). However, an  
389 increase in river discharge may weaken the effect of the biogeophysical feedback owing to a  
390 decrease in phytoplankton. Therefore, when performing the quantitative evaluation of the AA  
391 using phytoplankton in the Arctic Ocean or by prospecting Arctic ecosystems, we suggest that  
392 precise forcings of the freshwater input and more realistic response of sea ice are needed for the  
393 accurate simulation of phytoplankton growth. In this respect, it should be mentioned that the  
394 model used in this study is known to underestimate summer sea ice (Griffies et al., 2011).  
395 Therefore, careful interpretation is needed because our results indicate that phytoplankton  
396 response to the river discharge strongly depends on the distribution of sea ice concentration both  
397 in the present and future. Furthermore, Li et al. (2009) showed that an increase in river discharge

398 does not lead to a change in total phytoplankton biomass but does lead to an increase in the small  
399 size of phytoplankton. Although TOPAZv2 assumes three different size distributions of  
400 phytoplankton, it only explicitly provides the total biomass of phytoplankton.

401 Note that the current state-of-art EMSs do not realistically capture the complex bio-  
402 geophysical feedback between the Arctic environment and ecosystem (Vancoppenolle et al.,  
403 2013; Tangliabue et al., 2021). Multi-model ensemble mean estimates of present and future  
404 climate simulation from CMIP6 are generally known to exhibit superior results compared to  
405 those from CMIP5. However, they exhibit even greater uncertainties with respect to many  
406 variables especially for the biogeochemistry category, i.e., biomass of phytoplankton (Tagliabue  
407 et al., 2021). Therefore, our results can be useful for improving future Arctic ecosystem response  
408 simulations.

409 Due to the expected permafrost thawing in the future, additional nutrients input by river  
410 discharge was considered in the future simulation of the Arctic environmental and ecosystem  
411 change (Fichot et al, 2013; Turetsky et al., 2019). An increase in river discharge nutrients may  
412 cause an increase in shelf break, which can also be found in observations from previous studies  
413 (Ardyna et al., 2017). Terhaar et al. (2021) considered nutrients not only from river water but  
414 also from coastal erosion. However, Wikner & Andersson (2012) showed that an increase in  
415 river discharge leads to a decrease in the phytoplankton biomass because of increased microbial  
416 production. This is mainly due to the negative effects of freshwater and total organic carbon  
417 discharge on phytoplankton growth, despite a concomitant increase in nitrogen and phosphorus  
418 discharge. The mechanisms by which nutrients affect additional river discharge become  
419 increasingly more complex. Therefore, future modeling studies should consider positive and  
420 negative effects using more sophisticated biogeochemical models and evaluate their impact.

421           Importantly, we did not consider the temperature of rivers due to global warming. Recent  
422 studies demonstrated that the river temperatures have been increasing globally (Liu et al., 2020).  
423 The temperatures of arctic rivers do not appear to rise remarkably, mostly because they consume  
424 heat energy for phase change. However, Park et al. (2020) suggested that an increase in river  
425 water temperature could cause positive feedback in the Arctic climate. In future research, we  
426 plan to quantify the sensitivity to the riverine heat with respect to studying the actual future  
427 climate.

428           We looked at the sensitivity of freshwater inflows only by river water. However, Brown  
429 et al. (2019) pointed out that an increase in precipitation may be more effective in Arctic Ocean  
430 desalination than an increase in river discharge. In addition, the Arctic Ocean may be further  
431 desalinated by Greenland glaciers, which were not considered in this study (Arrigo et al., 2017;  
432 Kwiatkowski et al., 2019). Notably, it will be of great importance to conduct additional research  
433 by combining several desalination processes in the Arctic Ocean, in addition to our current  
434 experiment.

#### 435 **Acknowledgments**

436 This research was a part of the project titled ‘Korea-Arctic Ocean Warming and Response of  
437 Ecosystem(K-AWARE, KOPRI, 1525011760)’, funded by the Ministry of Oceans and Fisheries,  
438 Korea. And, This work was supported by the National Research Foundation of Korea(NRF)  
439 grant funded by the Korea government (MEST) (NRF-2019R1A2C1005460).

#### 441 **References**

- 442  
443 Ardyna, M., Babin, M., Devred, E., Forest, A., Gosselin, M., Raimbault, P., & Tremblay, J. (2017). Shelf-basin  
444 gradients shape ecological phytoplankton niches and community composition in the coastal Arctic Ocean  
445 (Beaufort Sea). *Limnology and Oceanography*, 62(5), 2113–2132. <https://doi.org/10.1002/lno.10554>  
446 Ardyna, Mathieu, & Arrigo, K. R. (2020). Phytoplankton dynamics in a changing Arctic Ocean. *Nature Climate*  
447 *Change*, 10(10), 892–903. <https://doi.org/10.1038/s41558-020-0905-y>  
448 Arrigo, K. R., Perovich, D. K., Pickart, R. S., Brown, Z. W., van Dijken, G. L., Lowry, K. E., et al. (2012). Massive  
449 phytoplankton blooms under arctic sea ice. *Science*, 336(6087), 1408. <https://doi.org/10.1126/science.1215065>  
450 Arrigo, K. R., Perovich, D. K., Pickart, R. S., Brown, Z. W., van Dijken, G. L., Lowry, K. E., et al. (2014).  
451 Phytoplankton blooms beneath the sea ice in the Chukchi sea. *Deep-Sea Research Part II: Topical Studies in*  
452 *Oceanography*, 105, 1–16. <https://doi.org/10.1016/j.dsr2.2014.03.018>

- 453 Arrigo, K. R., van Dijken, G. L., Castelao, R. M., Luo, H., Rennermalm, Å. K., Tedesco, M., et al. (2017). Melting  
454 glaciers stimulate large summer phytoplankton blooms in southwest Greenland waters. *Geophysical Research*  
455 *Letters*, *44*(12), 6278–6285. <https://doi.org/10.1002/2017GL073583>
- 456 Booth, G., P. Raymond, and N.-H. Oh. 2007. LoadRunner. Software and website. New Haven: Yale University.  
457 <http://research.yale>.
- 458 Bring, A., Shiklomanov, A., & Lammers, R. B. (2017). Pan-Arctic river discharge: Prioritizing monitoring of future.  
459 *Earth's Future*, *5*(1), 72–92. <https://doi.org/10.1002/ef2.175>
- 460 Brown, N. J., Nilsson, J., & Pemberton, P. (2019). Arctic Ocean Freshwater Dynamics: Transient Response to  
461 Increasing River Runoff and Precipitation. *Journal of Geophysical Research: Oceans*, *124*(7), 5205–5219.  
462 <https://doi.org/10.1029/2018JC014923>
- 463 Cohen, J., Screen, J. A., Furtado, J. C., Barlow, M., Whittleston, D., Coumou, D., et al. (2014). Recent Arctic  
464 amplification and extreme mid-latitude weather. *Nature Geoscience*, *7*(9), 627–637.  
465 <https://doi.org/10.1038/ngeo2234>
- 466 Comiso, J. C. (2003). Warming trends in the Arctic from clear sky satellite observations. *Journal of Climate*, *16*(21),  
467 3498–3510. [https://doi.org/10.1175/1520-0442\(2003\)016<3498:WTITAF>2.0.CO;2](https://doi.org/10.1175/1520-0442(2003)016<3498:WTITAF>2.0.CO;2)
- 468 Coumou, D., di Capua, G., Vavrus, S., Wang, L., & Wang, S. (2018). The influence of Arctic amplification on mid-  
469 latitude summer circulation. *Nature Communications*, *9*(1), 1–12. <https://doi.org/10.1038/s41467-018-05256-8>
- 470 Delworth, T. L., Rosati, A., Anderson, W., Adcroft, A. J., Balaji, V., Benson, R., et al. (2012). Simulated Climate  
471 and Climate Change in the GFDL CM2.5 High-Resolution Coupled Climate Model. *Journal of Climate*, *25*(8),  
472 2755–2781. <https://doi.org/10.1175/JCLI-D-11-00316.1>
- 473 Dunne, J. P., Gnanadesikan, A., Sarmiento, J. L., & Slater, R. D. (2010). *Technical description of the prototype*  
474 *version (v0) of Tracers Of Phytoplankton with Allometric Zooplankton (TOPAZ) ocean biogeochemical model*  
475 *as used in the Princeton IFMIP \* model †*.
- 476 Dunne, J. P., John, J. G., Adcroft, A. J., Griffies, S. M., Hallberg, R. W., Shevliakova, E., et al. (2012). GFDL's  
477 ESM2 Global Coupled Climate–Carbon Earth System Models. Part I: Physical Formulation and Baseline  
478 Simulation Characteristics. *Journal of Climate*, *25*(19), 6646–6665. <https://doi.org/10.1175/JCLI-D-11-00560.1>
- 480 Dunne, J. P., John, J. G., Shevliakova, S., Stouffer, R. J., Krasting, J. P., Malyshev, S. L., et al. (2013). GFDL's  
481 ESM2 global coupled climate-carbon earth system models. Part II: Carbon system formulation and baseline  
482 simulation characteristics. *Journal of Climate*. <https://doi.org/10.1175/JCLI-D-12-00150.1>
- 483 Fichot, C. G., Kaiser, K., Hooker, S. B., Amon, R. M. W., Babin, M., Bélanger, S., et al. (2013). Pan-Arctic  
484 distributions of continental runoff in the Arctic Ocean. *Scientific Reports*, *3*, 1–6.  
485 <https://doi.org/10.1038/srep01053>
- 486 Frey, K. E., Moore, G. W. K., Cooper, L. W., & Grebmeier, J. M. (2015). Divergent patterns of recent sea ice cover  
487 across the Bering, Chukchi, and Beaufort seas of the Pacific Arctic Region. *Progress in Oceanography*.  
488 <https://doi.org/10.1016/j.pocean.2015.05.009>
- 489 Gnanadesikan, A., Dixon, K. W., Griffies, S. M., Balaji, V., Barreiro, M., Beesley, J. A., et al. (2006). GFDL's CM2  
490 Global Coupled Climate Models. Part II: The Baseline Ocean Simulation. *Journal of Climate*, *19*(5), 675–697.  
491 <https://doi.org/10.1175/JCLI3630.1>
- 492 Green, P. A., Vörösmarty, C. J., Meybeck, M., Galloway, J. N., Peterson, B. J., & Boyer, E. W. (2004). Pre-  
493 industrial and contemporary fluxes of nitrogen through rivers: A global assessment based on typology.  
494 *Biogeochemistry*, *68*(1), 71–105. <https://doi.org/10.1023/B:BIOG.0000025742.82155.92>
- 495 Griffies, S. M., Gnanadesikan, A., Dixon, K. W., Dunne, J. P., Gerdes, R., Harrison, M. J., et al. (2005). Formulation  
496 of an ocean model for global climate simulations. *Ocean Science*, *1*(1), 45–79. <https://doi.org/10.5194/os-1-45-2005>
- 498 Griffies, Stephen M., Winton, M., Donner, L. J., Horowitz, L. W., Downes, S. M., Farneti, R., et al. (2011). The  
499 GFDL CM3 Coupled Climate Model: Characteristics of the Ocean and Sea Ice Simulations. *Journal of*  
500 *Climate*, *24*(13), 3520–3544. <https://doi.org/10.1175/2011JCLI3964.1>
- 501 Haine, T. W. N., Curry, B., Gerdes, R., Hansen, E., Karcher, M., Lee, C., et al. (2015). Arctic freshwater export:  
502 Status, mechanisms, and prospects. *Global and Planetary Change*, *125*, 13–35.  
503 <https://doi.org/10.1016/j.gloplacha.2014.11.013>
- 504 Hegglin, M. I., D. Kinnison, D. Plummer, et al., Historical and future ozone database (1850-2100) in support of  
505 CMIP6, GMD, in preparation. <https://blogs.reading.ac.uk/ccmi/forcing-databases-in-support-of-cmip6/>
- 506 Holland, M. M., Serreze, M. C., & Stroeve, J. (2010). The sea ice mass budget of the Arctic and its future change as  
507 simulated by coupled climate models. *Climate Dynamics*, *34*(2), 185–200. <https://doi.org/10.1007/s00382-008-0493-4>

- 509 Holmes, R. M., McClelland, J. W., Peterson, B. J., Tank, S. E., Bulygina, E., Eglinton, T. I., et al. (2012). Seasonal  
510 and Annual Fluxes of Nutrients and Organic Matter from Large Rivers to the Arctic Ocean and Surrounding  
511 Seas. *Estuaries and Coasts*, 35(2), 369–382. <https://doi.org/10.1007/s12237-011-9386-6>
- 512 Holmese, R. M., Shiklomanov A. I., Suslova A., Tretiakov M., McClelland J. W., Spencer R. G. M. and Tank S.  
513 E. , 2018: River Discharge [in Arctic Report Card 2018], <https://www.arctic.noaa.gov/Report-Card>.
- 514 Horvat, C., Jones, D. R., Iams, S., Schroeder, D., Flocco, D., & Feltham, D. (2017). The frequency and extent of  
515 sub-ice phytoplankton blooms in the Arctic Ocean. *Science Advances*, 3(3).  
516 [https://doi.org/10.1126/SCIADV.1601191/SUPPL\\_FILE/1601191\\_SM.PDF](https://doi.org/10.1126/SCIADV.1601191/SUPPL_FILE/1601191_SM.PDF)
- 517 Kashiwase, H., Ohshima, K. I., Nihashi, S., & Eicken, H. (2017). Evidence for ice-ocean albedo feedback in the  
518 Arctic Ocean shifting to a seasonal ice zone. *Scientific Reports*, 7(1), 1–10. [https://doi.org/10.1038/s41598-](https://doi.org/10.1038/s41598-017-08467-z)  
519 [017-08467-z](https://doi.org/10.1038/s41598-017-08467-z)
- 520 Kattner, G., & Budéus, G. (1997). Nutrient status of the Northeast Water Polynya. *Journal of Marine Systems*, 10(1–  
521 4), 185–197. [https://doi.org/10.1016/S0924-7963\(96\)00070-X](https://doi.org/10.1016/S0924-7963(96)00070-X)
- 522 Kennel, C. F., & Yulaeva, E. (2020). Influence of Arctic sea-ice variability on Pacific trade winds. *Proceedings of*  
523 *the National Academy of Sciences of the United States of America*, 117(6), 2824–2834.  
524 <https://doi.org/10.1073/pnas.1717707117>
- 525 Kim, B. M., Son, S. W., Min, S. K., Jeong, J. H., Kim, S. J., Zhang, X., et al. (2014). *Weakening of the stratospheric*  
526 *polar vortex by Arctic sea-ice loss*. *Nature Communications* (Vol. 5). Nature Publishing Group.  
527 <https://doi.org/10.1038/ncomms5646>
- 528 Kim, H. J., & An, S. il. (2019). Impact of north atlantic freshwater forcing on the pacific meridional overturning  
529 circulation under glacial and interglacial conditions. *Journal of Climate*, 32(15), 4641–4659.  
530 <https://doi.org/10.1175/JCLI-D-19-0065.1>
- 531 Kug, J. S., Jeong, J. H., Jang, Y. S., Kim, B. M., Folland, C. K., Min, S. K., & Son, S. W. (2015). Two distinct  
532 influences of Arctic warming on cold winters over North America and East Asia. *Nature Geoscience*, 8(10),  
533 759–762. <https://doi.org/10.1038/ngeo2517>
- 534 Kwiatkowski, L., Naar, J., Bopp, L., Aumont, O., DeFrance, D., & Couespel, D. (2019). Decline in Atlantic Primary  
535 Production Accelerated by Greenland Ice Sheet Melt. *Geophysical Research Letters*, 46(20), 11347–11357.  
536 <https://doi.org/10.1029/2019GL085267>
- 537 Lehner, F., Deser, C., Maher, N., Marotzke, J., Fischer, E. M., Brunner, L., et al. (2020). Partitioning climate  
538 projection uncertainty with multiple large ensembles and CMIP5/6. *Earth System Dynamics*, 11(2), 491–508.  
539 <https://doi.org/10.5194/ESD-11-491-2020>
- 540 Lewis, K. M., van Dijken, G. L., & Arrigo, K. R. (2020). Changes in phytoplankton concentration now drive  
541 increased Arctic Ocean primary production. *Science*, 369(6500), 198–202.  
542 <https://doi.org/10.1126/science.aay8380>
- 543 Lim, H. G., Kug, J. S., & Park, J. Y. (2019a). Biogeophysical feedback of phytoplankton on Arctic climate. Part II:  
544 Arctic warming amplified by interactive chlorophyll under greenhouse warming. *Climate Dynamics*, 53(5–6),  
545 3167–3180. <https://doi.org/10.1007/s00382-019-04693-5>
- 546 Lim, H. G., Kug, J. S., & Park, J. Y. (2019b). Biogeophysical feedback of phytoplankton on the Arctic climate.  
547 Part I: Impact of nonlinear rectification of interactive chlorophyll variability in the present-day climate.  
548 *Climate Dynamics*, 52(9–10), 5383–5396. <https://doi.org/10.1007/s00382-018-4450-6>
- 549 Lim, H. G., Park, J. Y., Dunne, J. P., Stock, C. A., Kang, S. H., & Kug, J. S. (2021). Importance of Human-Induced  
550 Nitrogen Flux Increases for Simulated Arctic Warming. *Journal of Climate*, 34(10), 3799–3819.  
551 <https://doi.org/10.1175/JCLI-D-20-0180.1>
- 552 Liu, S., Xie, Z., Liu, B., Wang, Y., Gao, J., Zeng, Y., et al. (2020). Global river water warming due to climate  
553 change and anthropogenic heat emission. *Global and Planetary Change*, 193, 103289.  
554 <https://doi.org/10.1016/J.GLOPLACHA.2020.103289>
- 555 Li, W. K. W., McLaughlin, F. A., Lovejoy, C., & Carmack, E. C. (2009). Smallest algae thrive as the Arctic Ocean  
556 freshens. *Science (New York, N.Y.)*, 326(5952), 539. <https://doi.org/10.1126/SCIENCE.1179798>
- 557 Manizza, M., & Que, C. le. (2005). Bio-optical feedbacks among phytoplankton , upper ocean physics and sea-ice in  
558 a global model, 32(2), 2–5. <https://doi.org/10.1029/2004GL020778>
- 559 Maslanik, J. A., Fowler, C., Stroeve, J., Drobot, S., Zwally, J., Yi, D., & Emery, W. (2007). A younger, thinner  
560 Arctic ice cover: Increased potential for rapid, extensive sea-ice loss. *Geophysical Research Letters*, 34(24),  
561 2004–2008. <https://doi.org/10.1029/2007GL032043>
- 562 McClelland, J. W., Holmes, R. M., Dunton, K. H., & Macdonald, R. W. (2012). The Arctic Ocean Estuary.  
563 *Estuaries and Coasts*, 35(2), 353–368. <https://doi.org/10.1007/S12237-010-9357-3/FIGURES/8>

- 564 Milly, P. C. D., & Shmakin, A. B. (2002). Global modeling of land water and energy balances. Part II: Land-  
565 characteristic contributions to spatial variability. *Journal of Hydrometeorology*, 3(3), 301–310.  
566 [https://doi.org/10.1175/1525-7541\(2002\)003<0301:GMOLWA>2.0.CO;2](https://doi.org/10.1175/1525-7541(2002)003<0301:GMOLWA>2.0.CO;2)
- 567 Min, S. K., Zhang, X., & Zwiers, F. (2008). Human-induced Arctic moistening. *Science*, 320(5875), 518–520.  
568 <https://doi.org/10.1126/science.1153468>
- 569 Morel, A. (1988). Optical modeling of the upper ocean in relation to its biogenous matter content (case I waters).  
570 *Journal of Geophysical Research*, 93(C9), 10749. <https://doi.org/10.1029/jc093ic09p10749>
- 571 Nicolaus, M., Katlein, C., Maslanik, J., & Hendricks, S. (2012). Changes in Arctic sea ice result in increasing light  
572 transmittance and absorption, 39(December), 1–6. <https://doi.org/10.1029/2012GL053738>
- 573 Nummelin, A., Ilicak, M., Li, C., & Smedsrud, L. H. (2016). Consequences of future increased Arctic runoff on  
574 Arctic Ocean stratification, circulation, and sea ice cover. *Journal of Geophysical Research: Oceans*, 121(1),  
575 617–637. <https://doi.org/10.1002/2015JC011156>
- 576 Park, H., Watanabe, E., Kim, Y., Polyakov, I., Oshima, K., Zhang, X., et al. (2020). Increasing riverine heat influx  
577 triggers Arctic sea ice decline and oceanic and atmospheric warming. *Science Advances*, 6(45).  
578 [https://doi.org/10.1126/SCIADV.ABC4699/SUPPL\\_FILE/ABC4699\\_SM.PDF](https://doi.org/10.1126/SCIADV.ABC4699/SUPPL_FILE/ABC4699_SM.PDF)
- 579 Park, J. Y., Kug, J. S., Bader, J., Rolph, R., & Kwon, M. (2015). Amplified Arctic warming by phytoplankton under  
580 greenhouse warming. *Proceedings of the National Academy of Sciences of the United States of America*,  
581 112(19), 5921–5926. <https://doi.org/10.1073/pnas.1416884112>
- 582 Peralta-Ferriz, C., & Woodgate, R. A. (2015). Seasonal and interannual variability of pan-Arctic surface mixed layer  
583 properties from 1979 to 2012 from hydrographic data, and the dominance of stratification for multiyear mixed  
584 layer depth shoaling. *Progress in Oceanography*, 134, 19–53. <https://doi.org/10.1016/j.pocean.2014.12.005>
- 585 Perovich, D. K., Jones, K. F., Light, B., Eicken, H., Markus, T., Stroeve, J., & Lindsay, R. (2011). Solar partitioning  
586 in a changing Arctic sea-ice cover. *Annals of Glaciology*, 52(57 PART 2), 192–196.  
587 <https://doi.org/10.3189/172756411795931543>
- 588 Perovich, Donald K., Light, B., Eicken, H., Jones, K. F., Runciman, K., & Nghiem, S. v. (2007). Increasing solar  
589 heating of the Arctic Ocean and adjacent seas, 1979-2005: Attribution and role in the ice-albedo feedback.  
590 *Geophysical Research Letters*. <https://doi.org/10.1029/2007GL031480>
- 591 Peterson, B. J., Holmes, R. M., McClelland, J. W., Vörösmarty, C. J., Lammers, R. B., Shiklomanov, A. I., et al.  
592 (2002). Increasing river discharge to the Arctic Ocean. *Science*, 298(5601), 2171–2173.  
593 <https://doi.org/10.1126/science.1077445>
- 594 Serreze, M. C., Holland, M. M., & Stroeve, J. (2007). Perspectives on the Arctic's shrinking sea-ice cover. *Science*,  
595 315(5818), 1533–1536. [https://doi.org/10.1126/SCIENCE.1139426/ASSET/71946118-C52C-4E98-8AD9-1850C9B21345/ASSETS/GRAPHIC/315\\_1533\\_F3.JPEG](https://doi.org/10.1126/SCIENCE.1139426/ASSET/71946118-C52C-4E98-8AD9-1850C9B21345/ASSETS/GRAPHIC/315_1533_F3.JPEG)
- 596 Shiklomanov, A.I., R.M. Holmes, J.W. McClelland, S.E. Tank, and R.G.M. Spencer. 2021. Arctic Great Rivers  
597 Observatory. Discharge Dataset, Version 20210527. <https://www.arcticrivers.org/data>
- 598 Shu, Q., Qiao, F., Song, Z., Zhao, J., & Li, X. (2018). Projected Freshening of the Arctic Ocean in the 21st Century.  
599 *Journal of Geophysical Research: Oceans*, 123(12), 9232–9244. <https://doi.org/10.1029/2018JC014036>
- 600 Smith, D. M., Screen, J. A., Deser, C., Cohen, J., Fyfe, J. C., García-Serrano, J., et al. (2019). The Polar  
601 Amplification Model Intercomparison Project (PAMIP) contribution to CMIP6: Investigating the causes and  
602 consequences of polar amplification. *Geoscientific Model Development*, 12(3), 1139–1164.  
603 <https://doi.org/10.5194/gmd-12-1139-2019>
- 604 Stouffer, R. J., Yin, J., Gregory, J. M., Dixon, K. W., Spelman, M. J., Hurlin, W., et al. (2006). Investigating the  
605 causes of the response of the thermohaline circulation to past and future climate changes. *86th AMS Annual  
606 Meeting*.
- 607 Tagliabue, A., Kwiatkowski, L., Bopp, L., Butenschön, M., Cheung, W., Lengaigne, M., & Vialard, J. (2021).  
608 Persistent Uncertainties in Ocean Net Primary Production Climate Change Projections at Regional Scales  
609 Raise Challenges for Assessing Impacts on Ecosystem Services. *Frontiers in Climate*, 3, 149.  
610 <https://doi.org/10.3389/FCLIM.2021.738224/BIBTEX>
- 611 Terhaar, J., Torres, O., Bourgeois, T., & Kwiatkowski, L. (2020). Arctic Ocean acidification over the  
612 21<sup>st</sup> century co-driven by anthropogenic carbon increases and freshening in the  
613 CMIP6 model ensemble. *Biogeosciences Discussions*, 1–30. <https://doi.org/10.5194/bg-2020-456>
- 614 Terhaar, J., Lauerwald, R., Regnier, P., Gruber, N., & Bopp, L. (2021). Production Sustained By Rivers and Coastal  
615 Erosion. *Nature Communications*, 1–10. Retrieved from <http://dx.doi.org/10.1038/s41467-020-20470-z>
- 616 Tremblay, J. E., Raimbault, P., Garcia, N., Lansard, B., Babin, M., & Gagnon, J. (2014). Impact of river discharge,  
617 upwelling and vertical mixing on the nutrient loading and productivity of the Canadian Beaufort Shelf.  
618 *Biogeosciences*, 11(17), 4853–4868. <https://doi.org/10.5194/bg-11-4853-2014>

- 620 Turetsky, M. R., Jones, M. C., Walter Anthony, K., Olefeldt, D., Schuur, E. A. G., Koven, C., et al. (2019).  
621 Permafrost collapse is accelerating carbon release. *Nature*, *569*, 32–24.
- 622 Vancoppenolle, M., Bopp, L., Madec, G., Dunne, J., Ilyina, T., Halloran, P. R., & Steiner, N. (2013). Future arctic  
623 ocean primary productivity from CMIP5 simulations: Uncertain outcome, but consistent mechanisms. *Global*  
624 *Biogeochemical Cycles*, *27*(3), 605–619. <https://doi.org/10.1002/gbc.20055>
- 625 Wikner, J., & Andersson, A. (2012). Increased freshwater discharge shifts the trophic balance in the coastal zone of  
626 the northern Baltic Sea. *Global Change Biology*, *18*(8), 2509–2519. [https://doi.org/10.1111/J.1365-](https://doi.org/10.1111/J.1365-2486.2012.02718.X)  
627 [2486.2012.02718.X](https://doi.org/10.1111/J.1365-2486.2012.02718.X)
- 628 Yin, J., & Stouffer, R. J. (2007). Comparison of the Stability of the Atlantic Thermohaline Circulation in Two  
629 Coupled Atmosphere–Ocean General Circulation Models. *Journal of Climate*, *20*(17), 4293–4315.  
630 <https://doi.org/10.1175/JCLI4256.1>  
631

Supporting Information for

**Increasing Arctic River Discharge and Its Role for the Phytoplankton Responses  
in the Present and Future Climate Simulations**

**Junghyun Park<sup>1</sup>, Seong-Joong Kim<sup>2</sup>, Hyung-Gyu Lim<sup>3</sup>, Jong-Seong Kug<sup>4</sup>, Eun Jin Yang<sup>5</sup> and Baek-Min Kim<sup>1,\*</sup>**

<sup>1</sup>Division of Earth Environmental System Science Major of Environmental Atmospheric Sciences, Pukyong National University, Busan, 48513, South Korea

<sup>2</sup>Division of Atmospheric Sciences, Korea Polar Research Institute, 26 Songdomirae-ro, Incheon, 21990, South Korea

<sup>3</sup>Atmospheric and Oceanic Sciences Program, Princeton University, Princeton, NJ 08540, USA

<sup>4</sup>Division of Environmental Science and Engineering, Pohang University of Science and Technology (POSTECH), Pohang, 37673, South Korea

<sup>5</sup>Division of Ocean Sciences, Korea Polar Research Institute, 26 Songdomirae-ro, Incheon, 21990, South Korea

**Contents of this file**

Figures S1 to S4

**Figure S1.** (a) Annual mean Arctic salinity for each experiment. (b) Annual average Arctic sea surface height for each experiment. The solid blue line denotes the trend line.

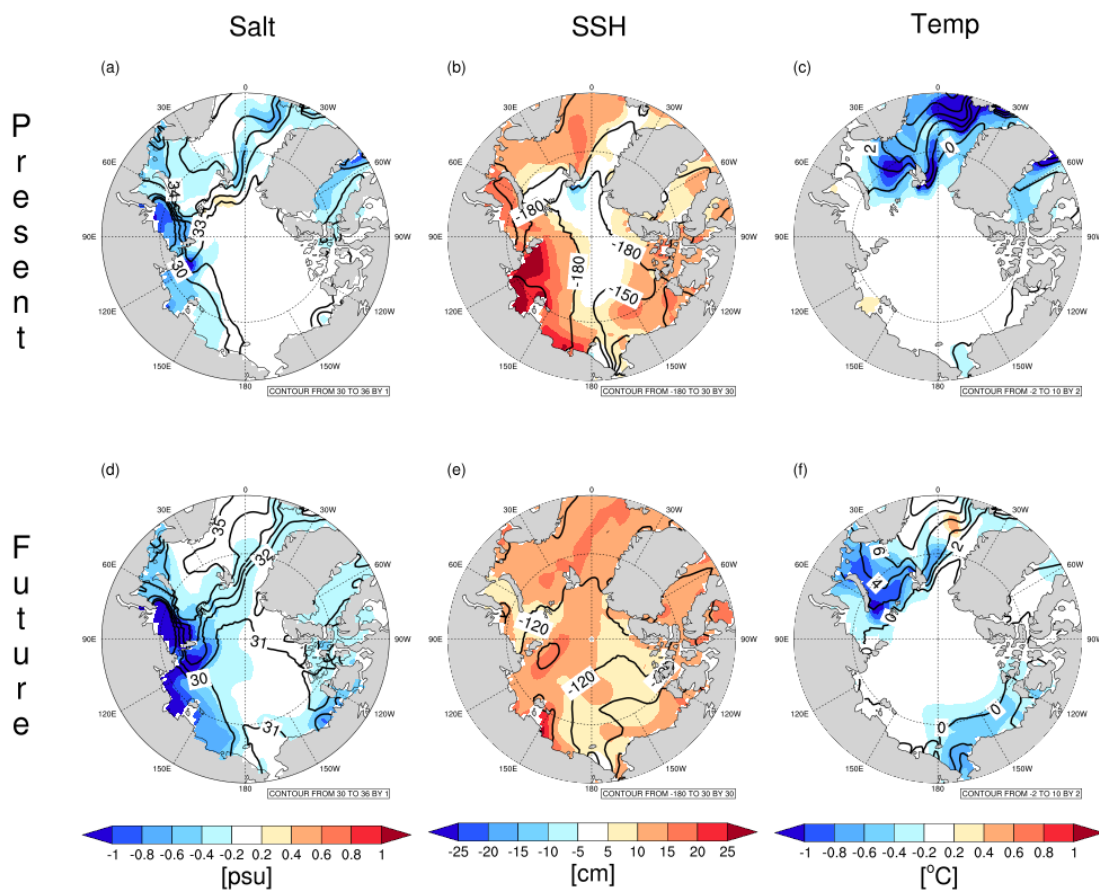


**Figure S2.** Impact of increased river discharge on April–July mean ocean environment variables in the present climate simulation. Difference between FWadd(P) and CTRL(P) for (a) salinity (salt) (shaded) and averaged salt on CTRL(P) (contour), (b) sea surface height (SSH), (c) ocean temperature (Temp). (d) Same as (a); (e) Same as (b); and (f) Same as (c), but for future climate simulation.



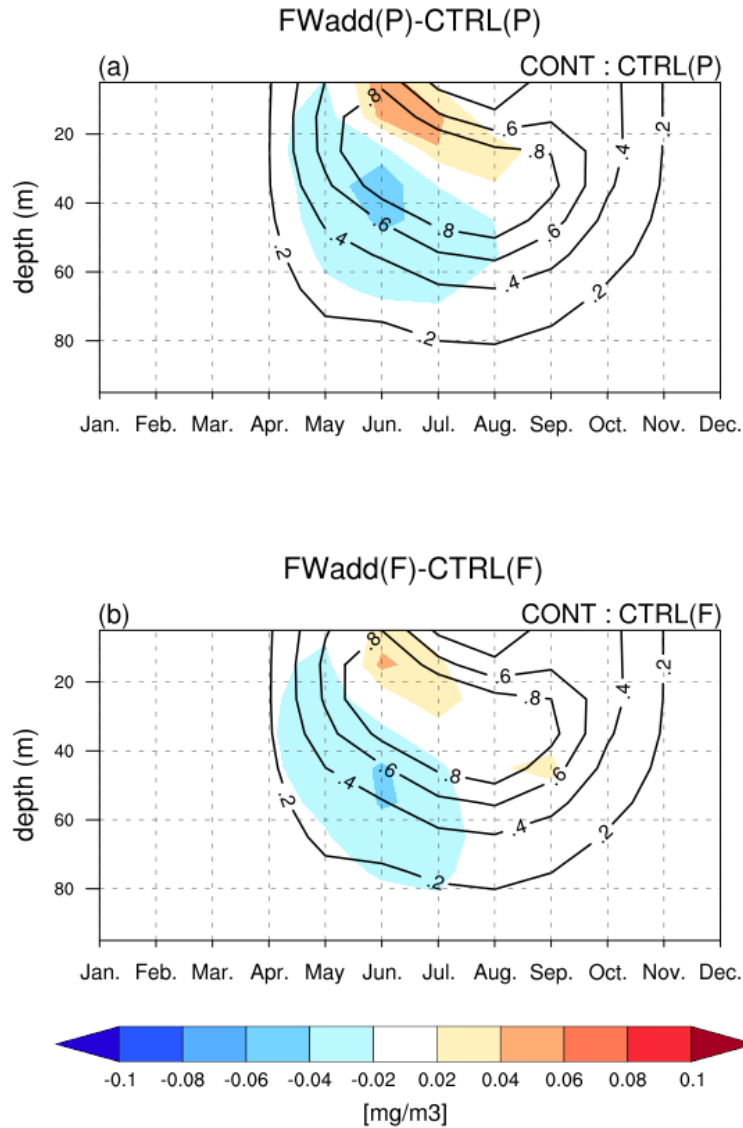


**Figure S3.** Impact of increased river discharge on the vertical structure of monthly chlorophyll concentration in the Arctic Ocean (>65° N). (a) Difference between FWadd(P) and CTRL(P) for chlorophyll concentration (shaded) and the averaged chlorophyll concentration. (b) Same as (a), except for FWadd(F) and CTRL(F).

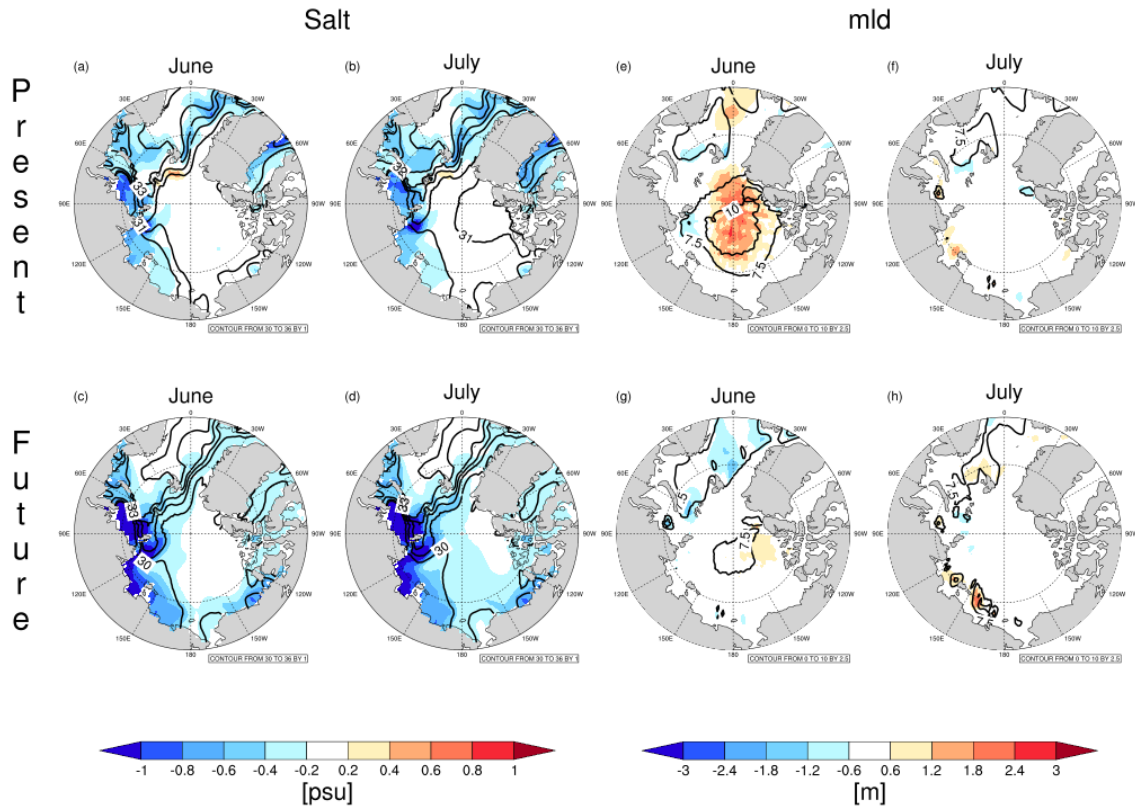


**Figure S4.** Impact of increased river discharge in summer mean salt and mixed layer (mld) in the present climate simulation. Difference between FWadd(P) and CTRL(P) of Salt (shaded) and the climatological salt on CTRL(P) (contour) in (a) June and (b) July. (c), (d) The same as (a) and (b), but for future climate. (e), (f) same as (a) and (b) but for mld. (g), (h) same as (e) and (f), but for future climate.